Morphological, ultrastructural and functional imaging of frozen/thawed and vitrified/warmed human ovarian tissue retrieved from oncological patients

Morphological, ultrastructural and functional imaging of frozen/thawed and vitrified/warmed human ovarian tissue retrieved from oncological patients

R. Fabbri, R. Vicenti, M. Macciocca, N.A. Martino, M.E. Dell'Aquila, G. Pasquinelli, A.M. Morselli-Labate, R. Seracchioli, R. Paradisi

Human Reproduction, Volume 31, Issue 8, August 2016, Pages 1838–1849, https://doi.org/10.1093/humrep/dew134

Abstract

STUDY QUESTION
Which is the best method for human ovarian tissue cryopreservation: slow freezing/rapid thawing (SF/RT) or vitrification/warming (V/W)?

SUMMARY ANSWER
The conventional SF/RT protocol used in this study seems to better preserve the morpho-functional status of human cryopreserved ovarian tissue than the used open carrier V/W protocol.

WHAT IS KNOWN ALREADY
Cryopreservation of human ovarian tissue is generally performed using the SF/RT method. However, reduction in the follicular pool and stroma damage are often observed. An emerging alternative procedure is represented by V/W which seems to allow the maintenance of the morphological integrity of the stroma.

STUDY DESIGN, SIZE, DURATION
This is a retrospective cohort study including six patients affected by oncological diseases and enrolled from January to December 2014.

PARTICIPANTS/MATERIALS, SETTING, METHODS

Ovarian tissue was laparoscopically harvested from the right and left ovaries and was cryopreserved using a routinary SF/RT protocol or a V/W method, involving tissue incubation in two solutions (containing propylene glycol, ethylene glycol and sucrose at different concentrations) and vitrification in an open system. For each patient, three pieces from each ovary were collected at the time of laparoscopy (fresh tissue) and after storage (SF/RT or V/W) and processed for light microscopy (LM) and transmission electron microscopy (TEM), to assess the morphological and ultrastructural features of follicles and stroma, and for laser scanning confocal microscopy (LSCM), to determine the functional energetic/redox stroma status. The preservation status of SF/RT and V/W ovarian tissues was compared with that of fresh ones, as well as between them.

MAIN RESULTS AND THE ROLE OF CHANCE

By LM and TEM, SF/RT and V/W samples showed cryodamage of small entity. Interstitial oedema and increased stromal cell vacuolization and chromatin clumping were observed in SF/RT samples; in contrast, V/W samples showed oocyte nuclei with slightly thickened chromatin and irregular shapes. The functional imaging analysis by LSCM revealed that the mitochondrial activity and intracellular reactive oxygen species levels were reduced both in SF/RT and in V/W samples compared with fresh samples. The study also showed progressive dysfunction of the mitochondrial activity going from the outer to the inner serial section of the ovarian cortex. The reduction of mitochondrial activity of V/W samples compared with fresh samples was significantly higher in the inner section than in the outer section.

LIMITATIONS, REASONS FOR CAUTION

The results report the bioenergetic and oxidative status assessment of fresh and cryopreserved human ovarian tissue by LSCM, a technique recently applied to tissue samples. The use of LSCM on human ovarian tissues after SF/RT or V/W is a new application that requires validation. The procedures for mitochondrial staining with functional probes and fixing are not yet standardized. Xenografting of the cryopreserved ovarian tissue in severe combined immunodeficient mice and *in vitro* culture have not yet been performed.

WIDER IMPLICATIONS OF THE FINDINGS

The identification of a cryopreservation method able to maintain the morpho-functional integrity of the ovarian tissue and a number of follicles comparable with those observed in fresh tissue might optimize results in clinical practice, in terms of recovery, duration of ovarian function and increased delivery outcomes after replanting. The SF/RT protocol allowed better morpho-functional tissue integrity than the V/W procedure.

STUDY FUNDING/COMPETING INTEREST(S)

Funding was provided by Fondazione del Monte di Bologna e Ravenna, Italy. Dr N.A.M. was granted by the project ONEV MIUR PONa3 00134-n.254/R&C 18 5 2011 and the project GR-2011-02351396 (Ministry of Health, Young Researchers Grant 2011/2012). There are no competing interests.

TRIAL REGISTRATION NUMBER

Clinical trial 74/2001/0 (approved:13 2 2002): ‘Pilot study on cryopreservation of human ovarian tissue: morphological and immunohistochemical analysis before and after cryopreservation’.

slow freezing, vitrification, light microscopy, transmission electron microscopy, laser scanning confocal microscopy, human ovarian tissue cryopreservation

Introduction

Recent advances in cancer diagnosis and new treatments have improved the survival of cancer patients. These therapies, however, lead to the reduction in primordial follicle pool which may result in infertility and, ultimately, in premature ovarian failure (Agarwal and Chang, 2007; Cvancarova et al., 2009; Jeruss and Woodruff, 2009; Schover, 2009). Ovarian tissue banking for future grafting is an attractive strategy to preserve the ovarian function of young women who suffer from malignant disease from the sterilizing

effects of chemo/radiotherapy. This is the only available option for patients who cannot delay the start of anti-cancer treatment, patients suffering from a hormonally sensitive cancer and for prepubertal girls who cannot undergo ovarian stimulation. In the last decade, the resumption of endocrine function has been reported in 80–90% of cases (Grynberg et al., 2012) and more than 60 healthy babies have been born after the transplantation of cryopreserved ovarian tissue in cancer survivors (Demeestere et al., 2015; Donnez and Dolmans 2015).

Cryopreservation of human ovarian tissue has generally been performed using the slow freezing/rapid thawing (SF/RT) method, even if a reduction in the follicular pool and an extensive damage in stromal cells have been reported in many studies (Navarro-Costa et al., 2005; Fabbri et al., 2010; Chang et al., 2011). An emerging alternative procedure is represented by vitrification/warming (V/W). The V/W procedure seems to have advantages compared with SF/RT, because the morphological integrity of the stromal component is better preserved than after SF/RT (Wang et al., 2008a,b; Xiao et al., 2010; Keros et al., 2009; Fabbri et al., 2014a). This method has been successfully applied to preserve human blastocysts and oocytes (Cobo et al., 2012), and for ovarian tissue, good results have been reported in rodents, domestic animals (Santana et al., 2012) and non-human primates (Amorim et al., 2011). Data on ovarian tissue vitrification in humans are still limited and conflicting, although two live births were recently reported after ovarian tissue V/W followed by in vitro activation of dormant follicles in patients with primary ovarian insufficiency (Suzuki et al., 2015).

Evaluation of aerobic metabolism may allow the identification of different types and extents of cell/tissue functional damage, and this may help in selecting better preserved samples for their subsequent use in vivo or in vitro. Although more frequently used to specifically target structural components and dynamic processes in fixed or living cells, the laser scanning confocal microscopy (LSCM) on tissue sections is becoming widespread for diagnostic applications (Rai and Dey, 2011). Recent studies report different settings and applications for precise pathology diagnoses (Robertson and Isacke, 2011; Lepreux et al., 2013; Kernohan and Bèrubè, 2014; Stempel et al., 2014; Pan et al., 2016). In the ovary, few studies have been reported to date in animal models

(Zucker and Jeffay, 2006; Faron et al., 2015). In humans, Rahimi and colleagues have analysed, by LSCM, the effects of different V/W protocols on ovarian tissue reactive oxygen species (ROS) and apoptosis (Rahimi et al., 2003) and followed the re-vascularization of ovarian tissue after SF/RT or V/W and transplantation to severe combined immunodeficient (SCID) mice (Rahimi et al., 2010), whereas Talevi and colleagues have assessed, by LSCM, the viability of ovarian tissue after slush nitrogen vitrification (Talevi et al., 2016). In our unit, LSCM has been used to monitor the preservation status of cryopreserved (SF/RT versus fresh) human ovarian tissue from cancer patients by assessing its bioenergetic/oxidative status in association with morphological and ultrastructural analysis by light microscopy (LM) and transmission electron microscopy (TEM) (Fabbri et al., 2014b).

In this study, to identify the best method of cryopreservation, the ovarian cortex retrieved from oncological patients was cryopreserved by SF/RT and V/W protocols. For each patient, the preservation status of the ovarian tissues cryopreserved using the two methods was compared with a fresh specimen, as well as between them using LM, TEM and LSCM.

Materials and Methods

Patients

Human ovarian tissue was collected from six patients aged 14–34 years (mean age ± SD: 24.5 ± 9.3 years), affected by Hodgkin lymphoma (two patients), breast cancer (two patients), brain tumour (one patient) and medulloblastoma (one patient). All subjects were referred to the Gynaecology and Pathophysiology of Human Reproductive Unit, S. Orsola-Malpighi University Hospital, Bologna, Italy for cryopreservation of ovarian tissue before chemotherapy and radiotherapy.

Ovarian tissue collection

Ovarian tissue was laparoscopically collected from the right and left ovaries. For each patient, three fresh pieces (1–3 mm) from each ovary were processed for LM, TEM and

LSCM analysis at the time of laparoscopy (fresh tissue). The remaining tissue was cryopreserved using SF/RT or V/W protocols. After storage for each patient, three pieces for each cryopreservation procedure were processed for the three imaging methods (LM, TEM and LSCM).

Cryopreservation procedures

SF/RT procedures

Samples were cryopreserved using our modified SF/RT protocols (Fabbri et al., 2010). In brief, ovarian samples were immersed into a ‘maintaining solution’ consisting of Dulbecco's phosphate-buffered saline (DPBS; Gibco®, Life Technologies, Paisley, Scotland) to which 10% heat-inactivated human serum (HS) was added (provided by the Transfusion Centre of S. Orsola-Malpighi Hospital). The ovarian cortex was cleaned of medulla, cut into slices 1.5 × 0.3 × 0.2 cm with a scalpel blade and placed in cryovials (Intermed Nunc Cryotubes, Denmark) containing the ‘freezing solution’ consisting of 1.26 mol/l 1,2-propanediol (PROH—Fluka Chemical, Sigma Aldrich, SrL, Milan, Italy), 0.175 mol/l sucrose (Fluka Chemical, Sigma Aldrich, SrL) with 30% of HS in DPBS, and transferred to a rolling system (Continents instrument, Amityville, NY) at 4°C for 1 h. The cryovials were transferred into a programmable freezer (Planer Kryo 10/1,7 Series III, SAPIO Life, Milan, Italy), allowing the gradual reduction of the temperature from 0 to −140°C. Then, the cryovials were transferred to cryogenic containers containing liquid nitrogen and stored until thawing. To thaw, the cryovials were air–warmed for 30 s and then immersed into 37°C water bath for 2 min. The cryoprotectants were removed at 4°C by four-stepwise dilution: (i) 0.76 mol/l PROH, 0.175 mol/l sucrose, 30% HS in DPBS for 5 min; (ii) 0.26 mol/l PROH, 0.175 mol/l sucrose, 30% HS in DPBS for an additional 5 min; (iii) 0.175 mol/l sucrose, 30% HS in DPBS for 10 min and, finally, (iv) DPBS supplemented with 30% HS at 4°C.

V/W procedures

Samples were cryopreserved according to our previously published V/W protocol (Fabbri et al., 2014a). Briefly, ovarian samples immersed in ‘maintaining solution’

consisting of DPBS with 10% of HS were cleaned of medulla and cut into slices 1.5 × 0.5 × 0.2 cm with a scalpel blade. The ovarian slices were transferred into a pre-cooled plastic cryovial containing the ‘equilibration solution’, consisting of 2 M propylene glycol (Fluka Chemical, Sigma Aldrich, SrL), 3 M ethylene glycol (Fluka Chemical, Sigma Aldrich, SrL), 0.2 M sucrose, 15% HS in DPBS, and were placed on a rolling system at 4°C for 30 min. Subsequently, each sample was transferred into a cryovial containing the ‘vitrification solution’, consisting of 3 M propylene glycol, 5 M ethylene glycol, 0.5 M sucrose, 15% HS in DPBS and again put onto a rolling system at 4°C for 30 min. Then, each sample was loaded in 200 µl of ‘vitrification solution’ onto an open plastic home-made support (diameter 0.8 cm; Fig. 1A) and quickly immersed into decontaminated liquid nitrogen. After that, the plastic support containing the sample was placed in an empty cryovial and stored into liquid nitrogen until warming (Fig. 1B). To warm the tissue, the plastic support was released from the cryovial, exposed to room temperature for 30 s and then immersed in a ‘warming solution’, consisting of 1 M sucrose, 15% HS in DPBS, for 1 min at 39°C, allowing the complete removal of the ice sleeve surrounding the sample, thus avoiding cryoprotectant dilutions in warming solutions. Subsequently, the cryoprotectant was removed at 4°C by a two-stepwise dilution of sucrose: (i) 0.5 M sucrose, 15% HS in DPBD for 3 min and (ii) 0.25 M sucrose, 15% HS in DPBS for 3 min. Finally, the warmed sample was rinsed two times at 4°C for 1 min in preequilibrated α-minimal essential medium (α-MEM, Sigma Aldrich SrL) supplemented with penicillin/streptomycin (0.1 mg/ml) and 10% HS.

Figure 1

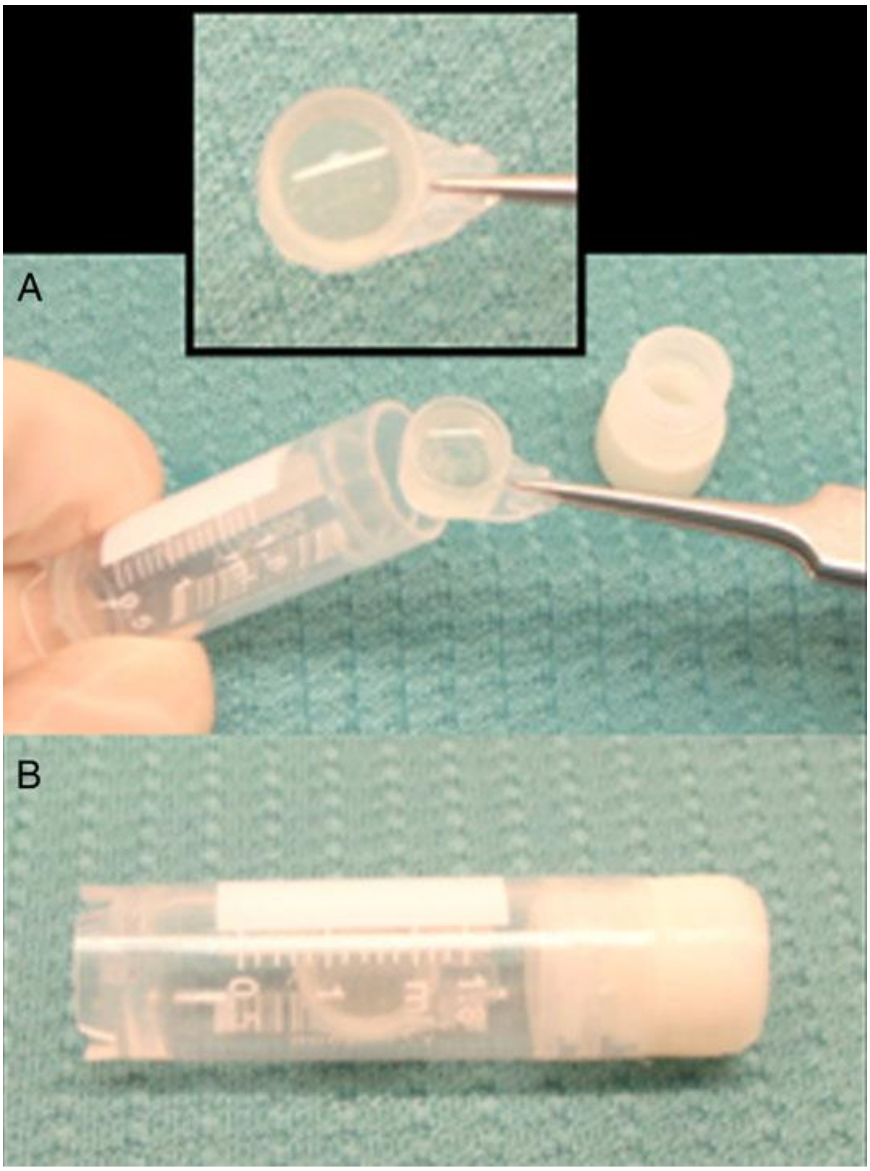

(A) Home-made plastic support for human ovarian tissue vitrification. (B) Plastic support placed in an empty cryovial for storage.

Light and transmission electron microscopy

A qualitative analysis of ovarian tissue was performed by histological and ultrastructural methods. Tissue pieces were embedded in paraffin blocks for LM. After deparaffination, four to six random sections of 4 µm thickness were stained with haematoxylin and

eosin. Sections were initially observed under a ×10 magnification microscope to detect artefacts and then observed at ×25 to assess developmental follicle stage according to Gougeon (1996), follicular density (follicle number per mm2 of the overall section area), follicle preservation and stromal integrity. Sections were observed in a blind fashion by two different operators in a Leitz Diaplan light microscope equipped with CCD JVC video camera (Leitz Diaplan, Wetzlar, Germany) and digitalized images were analysed with the Image ProPlus software (MediaCybernetics, Rockville, USA). For TEM, tissue samples were fixed in a freshly prepared 4% paraformaldehyde solution in 0.1 mol/l sodium cacodylate buffer (pH 7.4) overnight at 4°C. After 1% osmium tetroxide post-fixation and alcohol dehydration, samples were embedded in Araldite epoxy resin (Fluka, Buchs, Switzerland) and then sectioned with an ultramicrotome (Ultracut; Reichert, Wien, Austria). Sections of 60 nm thickness were collected on 200 mesh grids, stained with uranyl acetate followed by lead citrate and viewed using a Philips 410T transmission electron microscope at 80 kV, to evaluate the ultrastructural features of oocytes and granulosa and stromal cells, according to the criteria by Fabbri *et al.* (2010).

Confocal laser scanning microscopy

Mitochondria and ROS, and nuclear chromatin staining

Qualitative and quantitative analyses were performed by LSCM according to Fabbri *et al.* (2014b), to detect the bioenergetic (mitochondrial pattern and activity) and oxidative (intracellular ROS localization and levels) states of ovarian follicles and stroma before and after the cryopreservation procedures.

Fresh, thawed and warmed tissue samples were immediately washed in DPBS solution with 10% HS and incubated for 45 min in DPBS 10% HS with 280 nmol/l MitoTracker Orange CMTMRos (M7510; Molecular Probes, Oregon, USA) at 37°C under 6% CO_2 to detect and localize actively respiring mitochondria. The cell-permeant probe contains a thiol-reactive chloromethyl moiety. Once the MitoTracker probe accumulates in the mitochondria, it can react with accessible thiol groups on peptides and proteins to form an aldehyde-fixable conjugate. This cell-permeant probe is readily sequestered only by

actively respiring organelles depending on their oxidative activity (Martino *et al.*, 2013). After incubation with the mitochondria-specific probe, samples were washed three times in DPBS with 1% HS and incubated for 45 min in DPBS 1% HS with 10 µmol/l 2′,7′-dichlorodihydrofluorescein diacetate (DCDHF DA, D6883; Sigma Aldrich, Oakville, Ontario) to detect and localize intracellular sources of ROS. The non-ionized DCDHF DA is membrane permeant and therefore is able to diffuse readily into cells. Once within the cell, the acetate groups are hydrolysed by intracellular esterase activity forming 2′,7′-DCDHF which is polar and thus trapped within the cell. DCHF fluoresces when it is oxidized by H_2O_2 or lipid peroxides to yield 2′,7′-dichlorofluorescein (DCF). The level of DCF produced within the cells is linearly related to that of peroxides present and thus its fluorescent emission provides a measure of the peroxide levels (Martino *et al.*, 2013).

After incubation, samples were washed three times in prewarmed DPBS without HS and fixed overnight at 4°C in 2% formaldehyde solution in DPBS. Then, the samples were dehydrated in ethanol and xylene, embedded in paraffin and cut at 50 µm thickness. Three serial sections (Section 1: outer; Section 2: middle; Section 3: inner) for each experimental condition (fresh, SF/RT and V/W) were deparaffinized and covered with 3/1 glycerol/DPBS containing 2.5 mg/ml Hoechst 33258 for nuclear chromatin and apoptotic index evaluation. Negative controls were performed without the two specific mitochondrial and ROS probes.

Qualitative assessment of nuclear chromatin, mitochondrial distribution pattern and intracellular ROS localization

The nuclear chromatin pattern of oocytes, granulosa and stromal cells was observed under a Nikon Eclipse 600 fluorescent microscope (Nikon, Melville, New York) equipped with B2A (346 nm excitation/460 nm emission) filter at ×400 magnification. For the mitochondrial distribution pattern and intracellular ROS localization, ovarian tissue was observed at ×630 magnification under oil immersion with a Nikon C1/TE2000-U laser scanning confocal microscope (Nikon). A helium/neon laser ray at 543 nm and the G-2A filter (551 nm exposure and 576 nm emission) were used to identify the MitoTracker Orange CMTMRos. An argon ion laser ray at 488 nm and the B-2A filter (495 nm exposure and 519 nm emission) were used to identify the DCF. Scanning was

conducted with a series of 25 optical planes from the top to the bottom of the samples with a step size of 0.70 μm to allow three-dimensional distribution analysis.

Quantification of MitoTracker Orange CMTMRos and DCF fluorescence intensity

The quantification of MitoTracker Orange CMTMRos and DCF fluorescence intensities was performed at ×40 magnification. Excitation/emission was the same as described earlier, and imaging was performed using the EZ-C1 Gold Version 3.70 software platform for the Nikon C1 confocal microscope (Nikon). The intermediate focal plane was chosen for each of the three experimental conditions, and for each of the three serial slices (outer, middle and inner). Nine randomly selected regions of interest (50 000 μm^2) were drawn to measure the fluorescence intensity derived from the ovarian tissue. Parameters related to fluorescence intensity, such as laser energy, signal detection (gain) and pinhole size, were maintained at constant values for all measurements.

The analysis of the effects of cryopreservation procedures on bioenergetic/oxidative status of ovarian stromal tissue was performed on 162 data points to cover each experimental condition. Three serial sections, for each of the triplets of experimental conditions (fresh, SF/RT and V/W), for each of the six patients were analysed. For each serial section, nine regions of interest (ROIs) were selected as located in a chessboard manner (one in the centre, four at the corners of the innermost zone and four on the sides of the outer zone): 27 samples were available for each of the six patients, for each experimental condition.

Ethics

The cryopreservation protocol was approved by the Ethics Committee of S. Orsola-Malpighi Hospital (74/2001/O) and the study protocol conforms to the ethical guidelines of the ‘World Medical Association Declaration of Helsinki—Ethical Principles for Medical Research Involving Human Subjects’ adopted by the 18th WMA General Assembly, Helsinki, Finland, June 1964. Written informed consent was obtained from each patient.

Statistics

Mean, standard deviation and frequencies were used as descriptive statistics. Data were analysed by means of the repeated measure analysis of variance (ANOVA). In particular, according to the aim of the study, mitochondrial activity and intracellular ROS levels were analysed by considering the differences of the two studied cryopreservation procedures versus the fresh tissue as the main within sample factor and by adjusting for the two between sample factors which took into account the experimental design (i.e. the six patients and the three serial sections). In each of these two ANOVAs, the simple effects of the cryopreservation procedures were evaluated by means of within-sample nested designs, whereas between sample nested designs were applied to evaluate the effects within each serial section. The comparison of pairs of serial sections was made by means of the simple contrast to avoid multiple comparisons. The interactions were also considered in the ANOVA design to compare the differences between the two cryopreservation procedures among pairs of serial sections. The effects estimated by ANOVA have been reported together with their SE and 95% confidence intervals. Two similar one-way repeated measure ANOVAs were also applied to analyse the mean percentage of intact follicles observed in the six patients, detected by light microscopy and epifluorescence analysis. Data were managed and analysed by means of the IBM SPSS Statistics package (version, 21; IBM Co., Armonk, NY, USA) and two-tailed *P*-values <0.05 were considered statistically significant.

Results

Light and transmission electron microscopy

A total of 892 follicles (250 from fresh, 232 from frozen/thawed and 410 from vitrified/warmed samples) were analysed by light microscopy. The follicle density was 3.28 ± 6.85/mm^2 in fresh, 4.12 ± 5.65/mm^2 in frozen/thawed and 3.84 ± 5.36/mm^2 in vitrified/warmed tissue. Overall, the majority of follicles were primordial and intermediary (96.5%), whereas the remaining were at more advanced maturation stages (3.5%). The percentages of well-preserved follicles (follicles having an oocyte nucleus with

dispersed chromatin, homogeneous cytoplasm with perinuclear localization of mitochondria aggregates and no vacuolization, and follicular cells allocated tightly around the oocyte) were comparable in all experimental conditions: 23.2 ± 8.3% for fresh, 24.3 ± 13.5% for frozen/thawed and 29.6 ± 10.8% for vitrified/warmed samples.

Fresh stromal cells had an oval-shaped nucleus with a finely dispersed chromatin and small cytoplasmic vacuoles. Follicles showed close adherence between the oocyte and granulosa cells with normal morphological appearance: the oocytes had many mitochondria located around the nucleus, homogenous cytoplasm and no vacuoles (Fig. 2A). SF/RT and V/W samples showed cryodamage of small entity: in SF/RT samples, interstitial oedema, increased stromal cell vacuolization and stromal chromatin clumping were observed; whereas V/W samples showed oocyte nuclei with slightly thickened chromatin and irregular shapes (Fig. 2E and I).

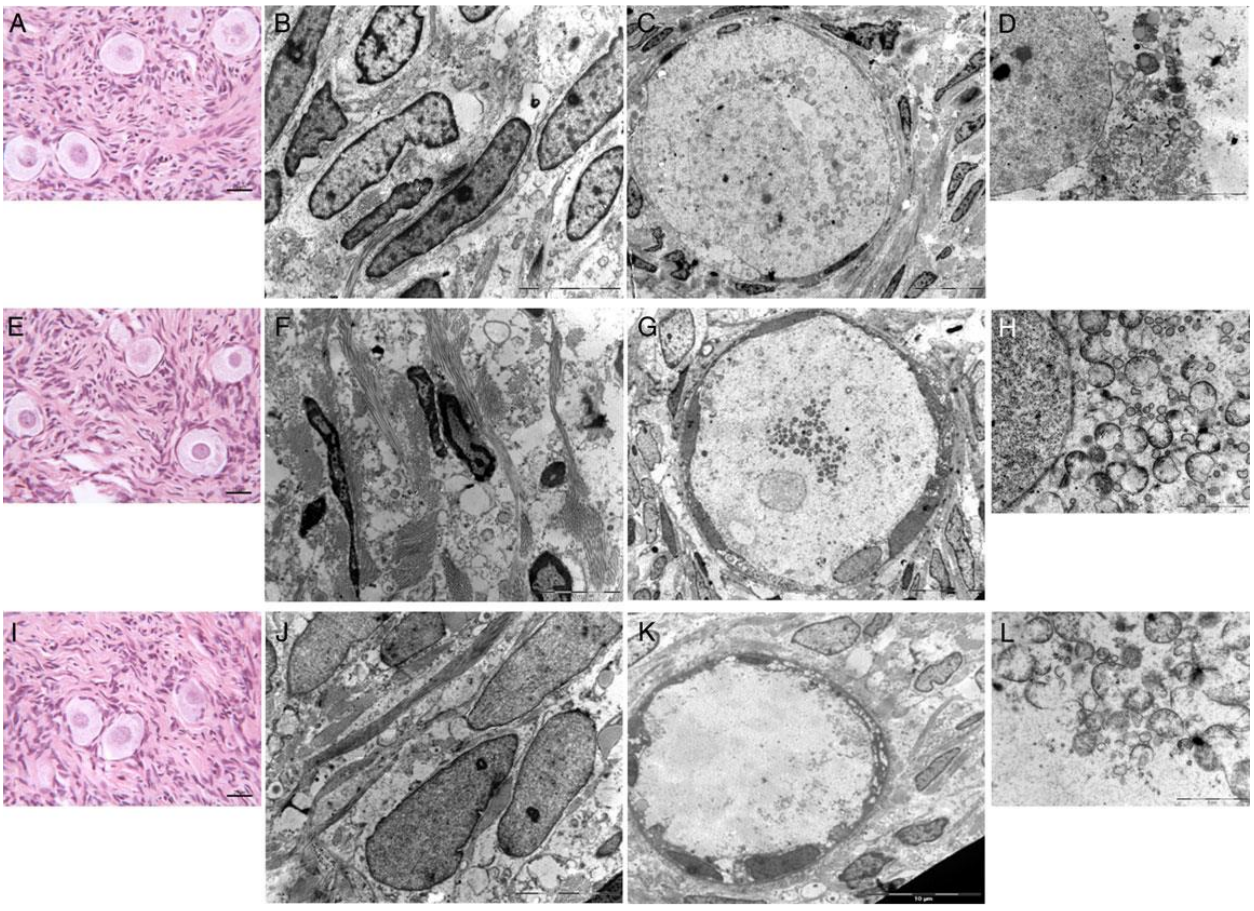

Figure 2

Light microscopy of follicles and stroma in fresh (A), frozen/thawed (E) and vitrified/warmed (I) ovarian samples (Bar 25 μm). TEM of follicles and stroma in fresh (B–D), frozen/thawed (F–H) and vitrified/warmed (J–L) ovarian samples. (B) Stroma showing stromal cells with dispersed nuclear chromatin without interstitial oedema or vacuolization (Bar 5 μm). (C) Fresh follicle showing a well-preserved oocyte and granulosa cells. The oocyte has a regularly shaped nucleus with intact membrane and mitochondria located around the nucleus (Bar 10 μm). (D) Rounded mitochondria clustered in the perinuclear region, smooth endoplasmic reticulum cisternae and lipid inclusions and lipofuscin bodies (Bar 5 μm). (F) Frozen/thawed stroma showing increased interstitial oedema and stromal cells with abundant chromatin clamping and cytoplasmic fragmentation (Bar 5μm). (G) Follicle showing a regularly shaped nucleus and finely dispersed chromatin, perinuclear mitochondria and well-preserved granulosa cells (Bar 10 μm). (H) Rounded intact mitochondria with few peripheral cristae and smooth endoplasmic reticulum cisternae (Bar 2 μm). (J) Stromal cells showing moderately dispersed chromatin and homogeneous cytoplasm with slight vacuolization (Bar 5 μm). (K) Vitrification-warmed follicle showing an irregular shape and clearing of the oocyte cytoplasm (Bar 10 μm). (L) Broken and swollen mitochondria scattered in the cytoplasm of the vitrified oocyte (Bar 2 μm).

By ultrastructural analysis, a total number of 63 follicles, equally distributed among fresh, SF/RT and V/W samples (21, 17, 25, respectively), were analysed. Fresh stroma showed spindle cells with moderately dispersed chromatin and homogeneous cytoplasm with a few empty vacuoles (Fig. 2B). Follicles contained large oocytes with regularly shaped nuclei, finely dispersed chromatin, nuclear pores and abundant cytoplasm. Mitochondria appeared typically rounded, with a low-density matrix and few peripheral cristae, clustered in the perinuclear region. The golgi apparatus was well developed and lipid inclusions and lipofuscin bodies were observed. A close adhesion between oocyte and granulosa cells was commonly seen. Granulosa cells showed flat nuclei, rod-shaped mitochondria, free ribosomes and scattered vacuoles in the cell cytoplasm (Fig. 2C and D).

The SF/RT stromal compartment showed increased interstitial oedema and stromal cell damage, consisting of rare pyknotic nuclei, or marked chromatin clumping and cytoplasmic fragmentation (Fig. 2F). Follicles showed regularly shaped nuclei and finely dispersed chromatin, perinuclear mitochondria and occasional clear vacuoles; granulosa cells were well-preserved (Fig. 2G and H).

V/W stromal cells showed moderately dispersed chromatin and homogeneous cytoplasm with slight vacuolization (Fig. 2J). Follicles contained an oocyte nucleus with slight irregular shape and slightly thickened chromatin; clear vacuoles and slight clarification in the oocyte cytoplasm were seen. Irregularly shaped, dark, broken or swollen mitochondria were found scattered in the cytoplasm or around the nucleus. Granulosa cells were adherent to oocyte (Fig. 2K and L).

Epifluorescence analysis of nuclear chromatin

Epifluorescence analysis using Hoechst staining showed similar mean ± SD percentages of intact follicles in the six patients comparable among fresh, SF/RT and V/W samples (55.4 ± 11.8%, 54.7 ± 17.3% and 54.9 ± 9.4%, respectively; $P = 0.946$ SF/RT versus fresh, $P = 0.949$ V/W versus fresh, $P = 0.940$ V/W versus SF/RT) and no apoptotic follicles or stromal cells were detected in any of the analysed samples.

Bioenergetic/oxidative status: qualitative analysis

A total of 125 follicles were analysed, 43 from fresh, 50 from SF/RT and 32 from V/W samples. All follicles were primordial or intermediary types. The LSCM analysis of follicles showed the presence of mitochondria- and ROS-specific fluorescence signals. Overall, perinuclear mitochondria aggregates were observed in fresh, SF/RT and V/W samples. The ROS signal was low in all analysed follicles. Merge images revealed that ROS colocalized with mitochondria. Aggregations of active mitochondria within the stromal cell cytoplasm were observed in fresh, SF/RT and V/W samples. In addition, DCF fluorescence was observed as uniformly distributed throughout the cytoplasm. No fluorescence was noted when the staining procedure was performed in medium depleted of mitochondria- and ROS-specific probes.

Bioenergetic/oxidative status: quantitative analysis

No quantitative analysis of mitochondria/ROS fluorescence intensity was performed on follicles, as a consequence of their resting stage and small cytoplasmic size.

The overall quantitative results of the effects of cryopreservation procedures on bioenergetic/oxidative state of ovarian tissue are shown in Fig. 3 and the results of the statistical analysis of mitochondrial activity and intracellular ROS levels of ovarian tissue are reported in Tables Ia and IIa, respectively. SF/RT samples showed a significant reduction of both mitochondrial activity (−37.5 ± 11.7; $P = 0.002$) and ROS levels (−71.9 ± 16.4; $P < 0.001$) compared with the fresh samples. A similar trend was observed comparing V/W and fresh samples for both mitochondrial activity (−102.7 ± 11.8; $P < 0.001$) and ROS levels (−159.8 ± 14.0; $P < 0.001$). The V/W samples had significantly lower values than the SF/RT ones for both parameters analysed (mitochondrial activity: −65.2 ± 9.3; $P < 0.001$; ROS levels: −87.9 ± 14.1; $P < 0.001$).

Table I
Results of the three-way ANOVA of mitochondrial activity level of ovarian tissue (ADU).

	Differences among cryopreservation procedures		
	SF/RT versus fresh	V/W versus fresh	V/W versus SF/RT
(a) Overall differences	−37.5 ± 11.7 (−60.6 to −14.3) *P* =0.002	−102.7 ± 11.8 (−126.1 to −79.3) *P* <0.001	−65.2 ± 9.3 (−83.6 to −46.8) *P* <0.001
(b) Differences within-section			
Serial Section 1 (Outer)	−33.3 ± 20.3 (−73.3 to 6.8) *P* =0.103	−78.1 ± 20.5 (−118.6 to −37.6) *P* <0.001	−44.8 ± 16.1 (−76.6 to −13.0) *P* =0.006

	Differences among cryopreservation procedures		
	SF/RT versus fresh	V/W versus fresh	V/W versus SF/RT
Serial Section 2 (Middle)	−21.2 ± 20.3 (−61.3 to 18.8) *P* =0.297	−92.6 ± 20.5 (−133.2 to −52.1) *P* <0.001	−71.4 ± 16.1 (−103.2 to −39.6) *P* <0.001
Serial Section 3 (Inner)	−57.9 ± 20.3 (−98.0 to −17.8) *P* =0.005	−137.3 ± 20.5 (−177.8 to −96.8) *P* <0.001	−79.4 ± 16.1 (−111.3 to −47.6) *P* <0.001
(c) Differences among sections			
Outer versus middle	−12.0 ± 28.7 (−68.7 to 44.6) *P* =0.675	14.6 ± 29.0 (−42.7 to 71.8) *P* =0.617	26.6 ± 22.8 (−18.4 to 71.6) *P* =0.245
Outer versus inner	24.6 ± 28.7 (−32.0 to 81.3) *P* =0.392	59.2 ± 29.0 (2.0 to 116.5) *P* =0.043	34.6 ± 22.8 (−10.4 to 79.6) *P* =0.130
Middle versus inner	36.7 ± 28.7 (−20.0 to 93.3) *P* =0.203	44.7 ± 29.0 (−12.6 to 102.0) *P* =0.125	8.0 ± 22.8 (−37.0 to 53.0) *P* =0.725

The mean ± SE estimates of the differences among cryopreservation procedures are shown together with their 95% confidence intervals within parentheses.

SF/RT, slow freezing/rapid thawing samples; V/W, vitrification/warming samples.

Table II

Results of the three-way ANOVA of intracellular ROS level of ovarian tissue (ADU).

	Differences among cryopreservation procedures		
	SF/RT versus fresh	V/W versus fresh	V/W versus SF/RT
(a) Overall differences	−71.9 ± 16.4 (−104.4 to −39.4) *P* <0.001	−159.8 ± 14.0 (−187.4 to −132.1) *P* <0.001	−87.9 ± 14.1 (−115.6 to −60.1) *P* <0.001
(b) Differences within-section			
Serial Section 1 (Outer)	−102.1 ± 28.5 (−158.3 to −45.8) *P* <0.001	−218.3 ± 24.3 (−266.2 to −170.4) *P* <0.001	−116.2 ± 24.4 (−164.4 to −68.1) *P* <0.001
Serial Section 2 (Middle)	−45.0 ± 28.5 (−101.3 to 11.2) *P* =0.116	−131.0 ± 24.3 (−178.9 to 83.0) *P* <0.001	−85.9 ± 24.4 (−134.1 to −37.8) *P* =0.001
Serial Section 3 (Inner)	−68.7 ± 28.5 (−124.9 to −12.4) *P* =0.017	−130.1 ± 24.3 (−178.0 to −82.1) *P* <0.001	−61.4 ± 24.4 (−109.5 to −13.2) *P* =0.013
(c) Differences among sections			
Outer versus middle	−57.1 ± 40.3 (−136.6 to 22.5) *P* =0.158	−87.4 ± 34.3 (−155.1 to −19.6) *P* =0.012	−30.3 ± 34.5 (−98.4 to 37.8) *P* =0.381
Outer versus inner	−33.4 ± 40.3 (−112.9 to 46.1) *P* =0.408	−88.2 ± 34.3 (−156.0 to −20.5) *P* =0.011	−54.9 ± 34.5 (−122.9 to 13.2) *P* =0.114

	Differences among cryopreservation procedures		
	SF/RT versus fresh	V/W versus fresh	V/W versus SF/RT
Middle versus inner	23.7 ± 40.3 (−55.9 to 103.2) *P* =0.558	−0.9 ± 34.3 (−68.7 to 66.9) *P* =0.979	−24.6 ± 34.5 (−92.6 to 43.5) *P* =0.477

The mean ± SE estimates of the differences among cryopreservation procedures are shown together with their 95% confidence intervals within parentheses.

SF/RT, slow freezing/rapid thawing samples; V/W, vitrification/warming samples

Figure 3

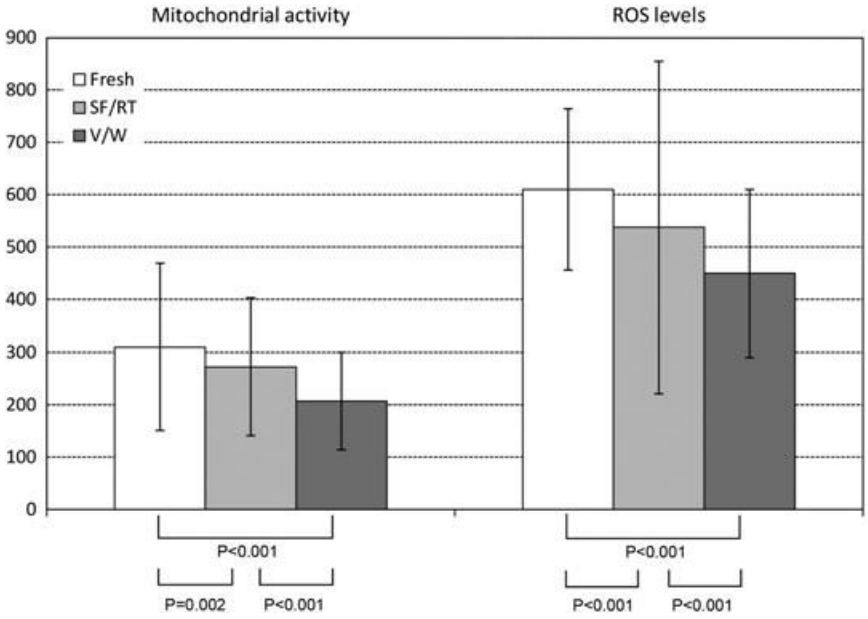

Mean ± SD of mitochondrial activity and intracellular ROS levels of ovarian tissue in fresh, SF/RT and V/W samples. Mitochondrial activity and ROS levels are expressed as MitoTracker Orange CMTM Ros and DCF fluorescence intensity in arbitrary densitometric units (ADU). There were 162 data points available to cover each experimental condition.

The within-section comparison among the three experimental conditions is shown in Figs 4 and 5 and the results of the statistical analysis of mitochondrial activity and

intracellular ROS levels of ovarian tissue are also reported in Tables Ib and IIb, respectively.

Figure 4

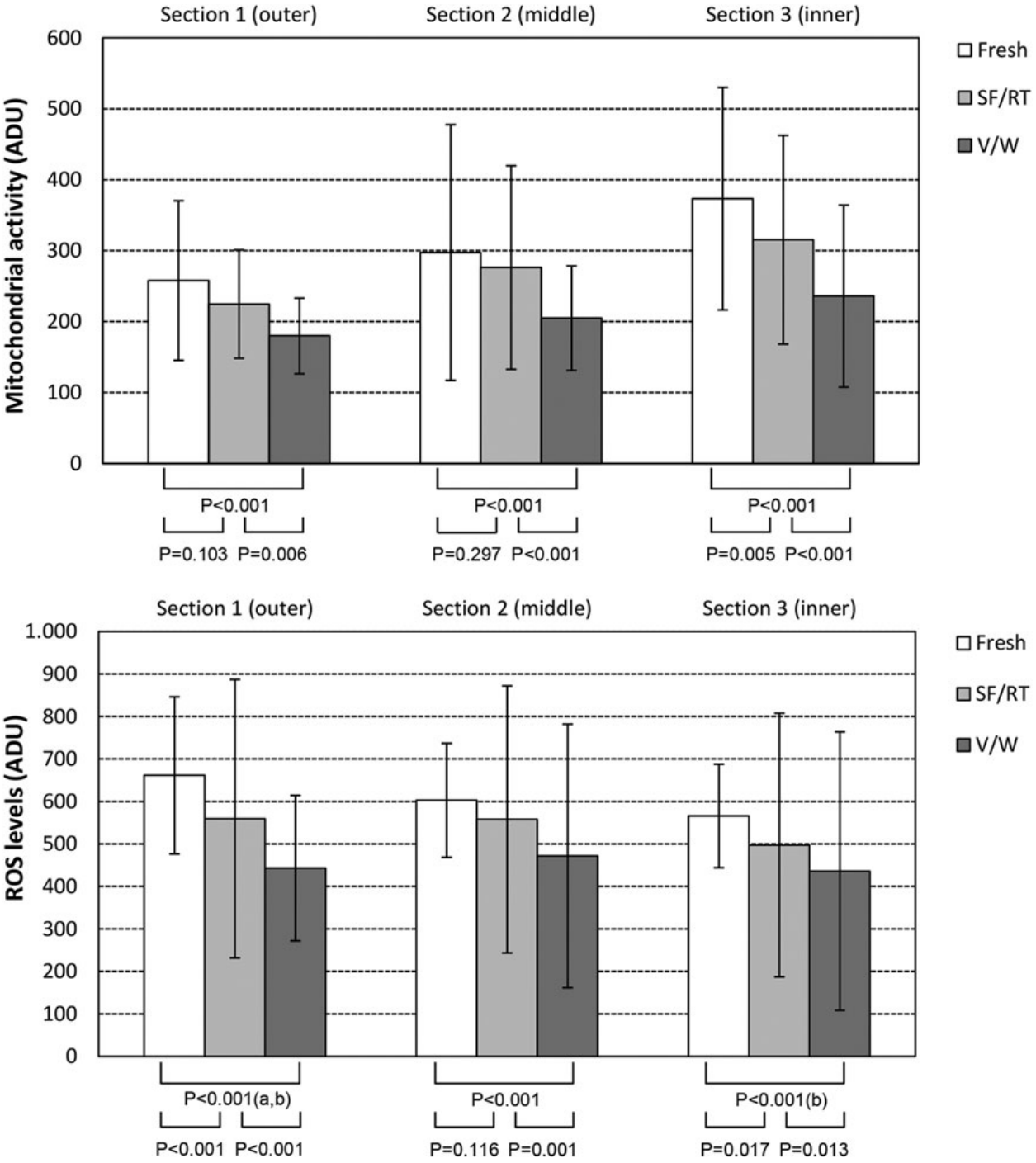

Mean ± SD of mitochondrial activity (upper panel) and intracellular ROS (lower panel) levels of ovarian tissue observed among the three serial sections (outer, middle and

inner) in fresh, SF/RT and V/W samples. Mitochondrial activity and ROS levels are expressed as MitoTracker Orange CMTM Ros and DCF fluorescence intensity in ADUs. There were 54 data points available for each serial section and for each experimental condition. Mitochondria activity: [a]The mean reduction of V/W versus the fresh tissue was significantly lower in Section 1 (−78.1) than in Section 3 (−137.3). Difference: 59.2 ± 29.0; $P = 0.043$. ROS levels: [a]The mean reduction of V/W versus the fresh tissue was significantly higher in Section 1 (−218.3) than in Section 2 (−131.0). Difference: −87.4 ± 34.3; $P = 0.012$. [b]The mean reduction of V/W versus the fresh tissue was significantly higher in Section 1 (−218.3) than in Section 3 (−130.1). Difference: −88.2 ± 34.3; $P = 0.011$.

Figure 5

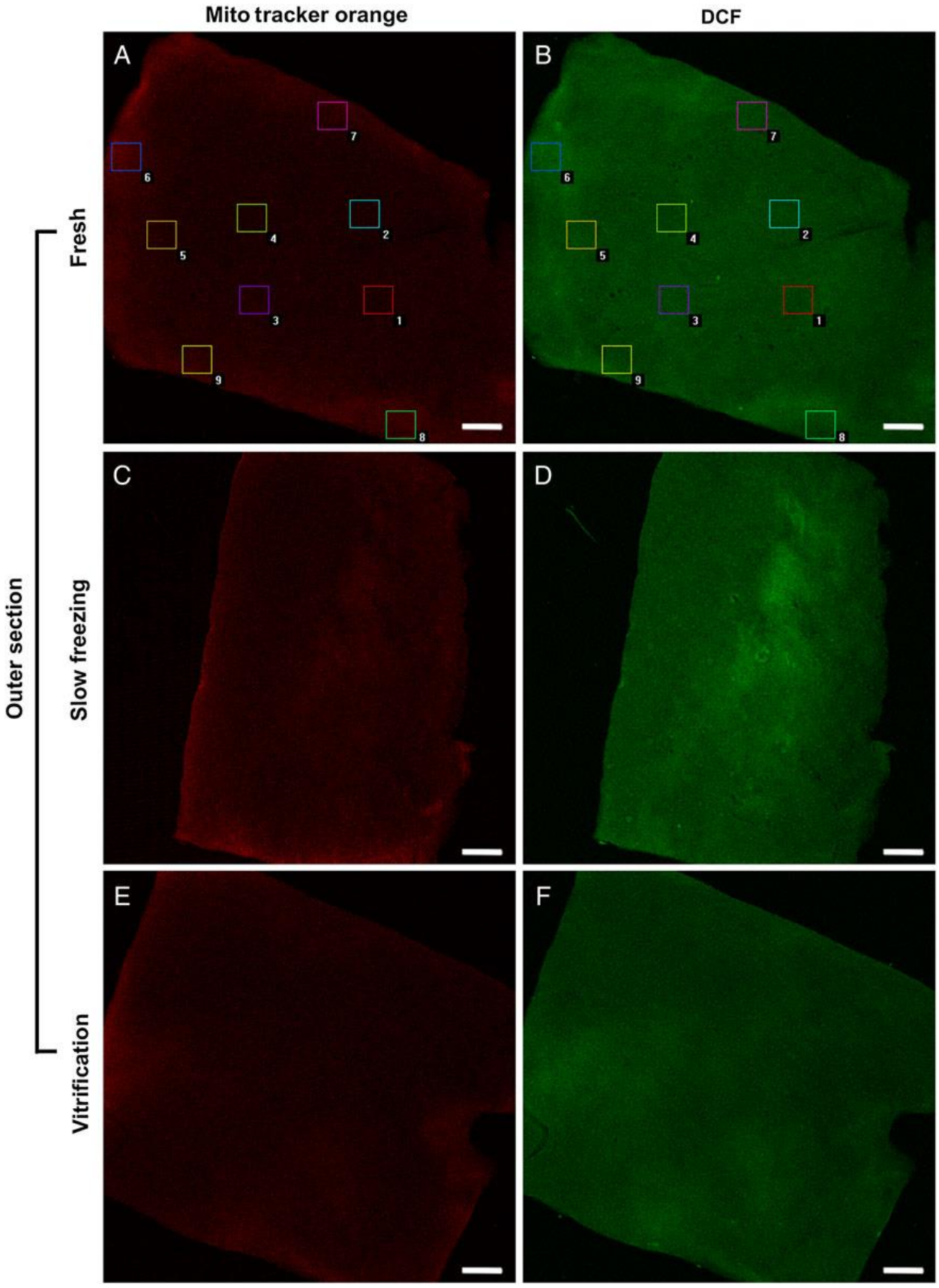
Mito tracker orange
DCF
A
B
C
D
E
F
Fresh
Slow freezing
Vitrification
Outer section
1
2
3
4
5
6
7
8
9

Photomicrographs of fresh, frozen/thawed and vitrified/warmed ovarian stromal samples assessed for their bioenergetic/oxidative potential. Representative confocal images showing mitochondrial activity (MitoTracker Orange) and intracellular ROS levels (DCF), of fresh (A and B), frozen/thawed (C and D) and vitrified/warmed (E and F) stromal ovarian tissue, are shown. Photomicrographs correspond to the outer section of the tissue. For quantification analysis, nine ROIs were selected, as shown in (A) and (B), as located in a chessboard manner. Decreased mitochondria activity and intracellular ROS levels can be seen in frozen/thawed (C and D) and vitrified/warmed (E and F) ovarian samples compared with the fresh one (A and B). Quantification data are shown in Fig. 3 (Bar 100 μm).

SF/RT had lower mitochondrial activity values than fresh tissue in the three sections, but these values reached the significant level only in the inner section (outer: −33.3 ± 20.3, $P = 0.103$; middle: −21.2 ± 20.3, $P = 0.297$; inner: −57.9 ± 20.3, $P = 0.005$). V/W values were significantly lower than both fresh (outer: −78.1 ± 20.5, middle: −92.6 ± 20.5, inner: −137.3 ± 20.5; $P < 0.001$ for the three sections) and SF/RT tissue values (outer: −44.8 ± 16.1, $P = 0.006$; middle: −71.4 ± 16.1, inner: −79.4 ± 16.1, $P < 0.001$ for both middle and inner) in all the three sections.

As far as the ROS levels were concerned, both SF/RT (outer: −102.1 ± 28.5, $P < 0.001$; middle: −45.0 ± 28.5, $P = 0.116$; inner: −68.7 ± 28.5, $P = 0.017$) and V/W tissues (outer: −218.3 ± 24.3, middle: −131.0 ± 24.3, inner: −130.1 ± 24.3; $P < 0.001$ for the three sections) had lower values than the fresh tissue in all sections, but the SF/RT tissues in the middle section did not reach the significance level. By comparing V/W and SF/RT tissues between themselves, the V/W samples had significantly lower values in all sections (outer: −116.2 ± 24.4, $P < 0.001$; middle: −85.9 ± 24.4, $P = 0.001$; inner: −61.4 ± 24.4, $P = 0.013$).

By comparing the bioenergetic/oxidative state of ovarian tissues among sections in any experimental condition (Fig. 4 and Tables Ic and IIc), the reductions of V/W versus the fresh tissue showed only some significant differences, whereas no significant differences were found between fresh and SF/RT tissues. In particular, the mean

reduction of mitochondrial activity of V/W versus the fresh tissue was significantly lower in the outer section (−78.1 ± 20.5) than in the inner section (−137.3 ± 20.5) with a difference of 59.2 ± 29.0 (P = 0.043). Similarly, the mean reduction of the ROS levels of V/W versus the fresh tissue was significantly higher in the outer section (−218.3 ± 24.3) than in both the middle section (−131.0 ± 24.3) and the inner section (−130.1 ± 24.3); these differences were −87.4 ± 34.3 (P = 0.012) and −88.2 ± 34.3 (P = 0.011), respectively.

Discussion

A major problem of cryopreservation procedures (either SF/RT or V/W) is proper assessment of the preservation status of ovarian tissue for its downstream purposes; different methods are used to investigate the morphological integrity as well as the functional status. In a previous study (Fabbri *et al.*, 2014b), LM, TEM and LSCM were applied as a combined efficient test to evaluate ovarian tissue preservation before and after cryopreservation, to highlight patient-specific variation on preservation of fresh and cryopreserved ovarian tissues. To overcome the effect of inter-patient variations, the comparison of the results of cryopreservation protocols was performed on the same patient. The assessment provided the identification of three functional conditions: tissues showing complete mitochondrial inactivity (worst preservation), or under oxidative stress conditions (i.e. tissue at risk of reduced follicular developmental potential; intermediate preservation), or normal functional conditions (best preservation).

In this study, fresh tissue showed good morphological and ultrastructural features associated with normal functional status. These features ensured a homogeneous baseline condition of fresh tissues before the application of the cryopreservation procedures.

LM evaluation showed that SF/RT and V/W samples maintained the same morphological characteristics of fresh samples, except for minor damage localized to stroma for SF/RT samples and in follicles for V/W samples.

TEM assessment confirmed observations obtained with LM as it highlighted that the stromal compartment of SF/RT samples showed increased interstitial oedema and cell damage, such as pyknotic nuclei or abundant chromatin clumping and cytoplasmic fragmentation. The V/W follicles had nuclei with slightly irregular shapes, clear vacuoles and slight clarification in the oocyte cytoplasm and mitochondria that were irregularly shaped, dark, broken or swollen. Probably, the causes of major damage in V/W samples may be related to the size of the samples and the device used in V/W protocols. In our V/W protocol, the size of the V/W samples was greater than that of the SF/RT samples: it is possible that the solutions used in this study were not able to penetrate the whole sample and to protect it from cryodamage. Data from the current literature show that the sample size has a strong influence on the tissue preservation status: small-sized specimens have been used in V/W protocols, with good results in terms of tissue preservation in the majority of studies (Amorim *et al.*, 2011). However, cutting the ovarian tissue in pieces that are too small causes the destruction of many follicles, leading to a reduction in the follicular reserve of the grafting pieces (Jeremias *et al.*, 2003). In the clinical practice, the best results in terms of live births have been obtained by transplanting pieces of at least 1 cm in length and 2 mm in width, cryopreserved by slow freezing/rapid thawing. It is known that the cryopreservation device also plays an important role towards the final outcome due to the cooling rate inside the tissue (Zhou *et al.*, 2010; Amorim *et al.*, 2011). Because of the absence of a certified device for human ovarian tissue vitrification, samples in this study were placed on a plastic home-made support with the medullar compartment facing the interior side of the support. Plastic is not a good temperature conductor: this could have caused sub-optimal reduction of the temperature with subsequent cryodamage.

To avoid the limitations of morphologic studies that are unable to give an indication of tissue functional integrity, we investigated the bioenergetic and oxidative status of fresh and cryopreserved human ovarian tissue by LSCM.

The functional imaging analysis revealed that mitochondrial activity and ROS levels were reduced both in SF/RT and in V/W samples compared with fresh samples. The

reduction of the two functional parameters was more pronounced in the V/W than in the SF/RT samples. The LSCM analysis of the bioenergetic/oxidative status of V/W samples indicates a severe cryopreservation-induced functional damage, with reduced mitochondrial oxidative phosphorylation activity associated with a decrease in the mitochondrial capacity to synthesize ROS.

Our study also showed differences of mitochondrial activity and ROS levels among the three serial sections. In particular, the reduction of mitochondrial activity in the inner section of V/W samples compared with fresh samples was significantly higher than in the outer section. For ROS levels, in the middle and inner sections, there were significantly lower reductions in V/W samples, compared with fresh ones, than in the outer section.

These data allow us to draw some conclusions: to assess the mitochondrial activity, the inner section (corresponding to the interface portion between the medullar and cortical tissue) must be excluded, thus limiting the analysis to the outer and/or middle sections (corresponding to the cortex of the ovary, a well-structured tissue containing follicular and stromal cells). The inner section was in direct contact with the plastic support in the V/W samples: this could explain the bad functional preservation identified at this level. The ultrastructural analysis confirmed these data; in fact, the follicular damage was found in the internal part of the samples, corresponding to the inner section of the samples prepared for LSCM analysis.

The significant reduction of mitochondria activity found in the inner section, both after SF/RT and V/W, represents a heavy cell/tissue damage as the mitochondrion is the core of cellular energy metabolism, being the site of most ATP generation (Cadenas and Davies, 2000; Brookes *et al.*, 2004). Moreover, such decay in mitochondrial activity was associated with significant reduction of ROS levels, even if not with the highest ROS reductions, which was observed in the outer section. This apparent discrepancy can be explained considering that mitochondrial activity and intracellular ROS levels are two independent variables, due to multiple intracellular mechanisms by which ROS are produced, both at mitochondrial level (Cadenas and Davies, 2000) and in other sub-

cellular compartments, such as peroxisomes, endoplasmic reticulum and the plasma membrane (Bae *et al.*, 2011). Further, our data are in line with previous studies inferring that ROS levels may show or not, weak or strong, positive or negative correlations with mitochondrial function (Kim *et al.*, 2013; Fedyaeva *et al.*, 2014).

Several studies on the comparison between SF/RT and V/W have been carried out in the current literature (Li *et al.*, 2007; Huang *et al.*, 2008; Wang *et al.*, 2008a,b; Isachenko *et al.*, 2009; Keros *et al.*, 2009; Rahimi *et al.*, 2010; Xiao *et al.*, 2010; Oktem *et al.*, 2011; Herraiz *et al.*, 2014; Klocke *et al.*, 2015; Sanfilippo *et al.*, 2015). However, the issue of whether vitrification is superior (whether it allows a better preservation status) to SF/RT for cryopreserved human ovarian tissue remains unsolved. The absence of clear results likely reflects either heterogeneity in the applied cryopreservation protocols and/or disparities in the methods employed to evaluate ovarian tissue quality. Isachenko *et al.* (2009) performed a study that compared the two main cryopreservation protocols, concluding that SF/RT is more promising than V/W. Subsequently, other authors obtained the same results: Rahimi *et al.* (2009) observed a higher percentage of apoptotic cells in V/W human ovarian tissues after grafting compared with SF/RT and Oktem *et al.* (2011) showed higher primordial follicle density and viability after SF/RT compared with V/W. Despite these promising data, other studies have failed to find any difference between these two cryopreservation procedures. Some authors reported that after *in vitro* culture of V/W and SF/RT human ovarian tissue, similar numbers of morphologically intact follicles, proportions of apoptotic cells and synthesis levels of estradiol were observed (Li *et al.*, 2007; Huang *et al.*, 2008, Klocke *et al.*, 2015, Sanfilippo *et al.*, 2015). Rahimi *et al.* (2010) reported that the SF/RT and V/W influence in the same manner follicle density and development during long-term *in vitro* culture and after xenografting in SCID mice. However, other authors have described better results applying the V/W protocol. Wang *et al.* (2008a,b) utilized very fine needles (NIV method) to manipulate the human and mouse ovarian tissue strips during vitrification to maximize the cooling rate; they showed that ultrastructure of the stromal cells and the viability of ovarian tissue were better preserved in NIV group than in the other groups. Keros *et al.* (2009) described comparable morphological preservation of human follicles after SF/RT and V/W

protocols followed by *in vitro* culture and a better morphological integrity for stromal cells after vitrification. Xiao *et al.* (2010) obtained a higher proportion of normal ultrastructure of granulosa cells and stromal cells and a reduction of TUNEL-positive primordial follicles and stromal cells using the NIV method with a lower concentration of cryoprotectants. Herraiz *et al.* (2014) demonstrated that human ovarian tissue vitrification does not affect the normal morphology, viability, proliferation and apoptosis of oocytes, follicles and blood vessel distribution after transplantation.

In agreement with Isachenko *et al.* (2009), Rahimi *et al.* (2009) and Oktem *et al.* (2011), in our study SF/RT appears more promising than V/W, for the lack of follicular cryodamage and for improved functional status. Of course, the imaging techniques used in this study cannot prove whether the cryodamage was reversible or not. Additional tests, such as *in vitro* culture or/and xenotransplantation, showing cryopreserved follicle survival and developmental potential, would be valuable tools in the application of ovarian tissue cryopreservation (Gook *et al.*, 2005; Wang *et al.*, 2016). Despite our findings that SF/RT seems to give better results than V/W, the real quality of the cryopreserved tissue can be assessed only after grafting. Further evidence of the feasibility of our SF/RT protocol was the follicular development in graft sites and the ovarian function recovery for more than 2 years after autotransplantation of ovarian cryopreserved tissue (Fabbri *et al.*, 2014c).

Our V/W protocol showed good preservation of the stromal compartment but damage in follicles, as evidenced by this study and our previously published study (Fabbri *et al.*, 2014a). These findings have not encouraged us to test follicle development by transplantation or *in vitro* culture. Therefore, further studies are necessary and essential to optimize the V/W protocol and if deciding to switch from conventional SF/RT to V/W for human ovarian tissue cryopreservation.

Authors' roles

R.F. and R.V.: designed the project, thawed the ovarian cortex, processed ovarian cortex for light, transmission and LSCM, acquired and interpreted data and wrote the manuscript. M.M.: thawed the ovarian cortex, processed ovarian cortex for light,

transmission and LSCM and contributed in the manuscript writing. G.P.: evaluated ovarian cortex processed for histological and ultrastructural analysis. N.A.M. and M.E.D.: evaluated ovarian cortex processed for LSCM, acquired and interpreted data and contributed in the manuscript writing. A.M.M.-L.: performed statistical analysis and contributed in the manuscript writing. R.P. and R.S.: contributed in designing the study and approved the manuscript.

Funding

Funding was provided by Fondazione del Monte di Bologna e Ravenna, Italy. N.A.M. was granted by the project ONEV MIUR PONa3 00134-n.254/R&C 18/05/2011 and the project GR-2011-02351396 (Ministry of Health, Young Researchers Grant 2011/2012).

Conflict of interest

The authors have no conflict of interest to declare.

References

Agarwal SK, Chang RJ. Fertility management for women with cancer. Cancer Treat Res 2007;138:15–27.
Amorim CA, Curaba M, Van Langendonckt A, Dolmans MM, Donnez J. Vitrification as an alternative means of cryopreserving ovarian tissue. Reprod Biomed Online 2011;23:160–186.
Bae YS, Oh H, Rhee SG, Yoo YD. Regulation of reactive oxygen species generation in cell signaling. Mol Cells 2011;32:491–509.
Brookes PS, Yoon Y, Robotham JL, AndersMW, Sheu SS. Calcium, ATP, and ROS: a mitochondrial love-hate triangle. Am J Physiol Cell Physiol 2004; 287:C817–C833.
Cadenas E, Davies KJ. Mitochondrial free radical generation, oxidative stress, and aging. Free Radic Biol Med 2000;29:222–230.
Chang HJ, Moon JH, Lee JR, Jee BC, Suh CS, Kim SH. Optimal condition of vitrification method for cryopreservation of human ovarian cortical tissues. J Obstet Gynaecol Res 2011;37:1092–1101.

Cobo A, de los Santos MJ, Castello` D, Ga´miz P, Campos P, Remohı´ J. Outcomes of vitrified early cleavage-stage and blastocyst-stage embryos in a cryopreservation program: evaluation of 3150 warming cycles. Fertil Steril 2012;98:1138–46.e1.
Cvancarova M, Samuelsen SO, Magelssen H, Fossa˚ SD. Reproduction rates after cancer treatment: experience from the Norwegian radium hospital. J Clin Oncol 2009;27:334–343.
Demeestere I, Simon P, Dedeken L, Moffa F, Tse´pe´lidis S, Brachet C, Delbaere A, Devreker F, Ferster A. Live birth after autograft of ovarian tissue cryopreserved during childhood.HumReprod 2015;30:2107–2109.
Donnez J, Dolmans MM. Ovarian cortex transplantation: 60 reported live births brings the success and worldwide expansion of the technique towards routine clinical practice. J Assist Reprod Genet 2015;32:1167–1170.
Fabbri R, Pasquinelli G, Keane D, Magnani V, Paradisi R, Venturoli S. Optimization of protocols for human ovarian tissue cryopreservation with sucrose, 1,2-propanediol and human serum. Reprod Biomed Online 2010;21:819–828.
Fabbri R, Vicenti R, Macciocca M, Pasquinelli G, Paradisi R, Battaglia C, Martino NA, Venturoli S. Good preservation of stromal cells and no apoptosis in human ovarian tissue after vitrification. Biomed Res Int 2014a;2014:673537.
Fabbri R, Vicenti R, Martino NA, Dell'Aquila ME, Pasquinelli G, Macciocca M, Magnani V, Paradisi R, Venturoli S. Confocal laser scanning microscopy analysis of bioenergetic potential and oxidative stress in fresh and frozen/thawed human ovarian tissue from oncologic patients. Fertil Steril 2014b;101:795–804.
Fabbri R, Pasquinelli G, Magnani V, Macciocca M, Vicenti R, Parazza I, Paradisi R, Battaglia C, Rossi S, Venturoli S. Autotransplantation of cryopreserved ovarian tissue in oncological patients: recovery of ovarian function. Future Oncol 2014c;10:549–561.
Faron J, Bernas´ T, Sas-Nowosielska H, Klag J. Analysis of the behavior of mitochondria in the ovaries of the earthworm Dendrobaenaveneta Rosa 1839. PLoS One 2015;10:e0117187.
FedyaevaAV, StepanovAV, Lyubushkina IV, Pobezhimova TP, Rikhvanov EG. Heat shock induces production of reactive oxygen species and increases inner mitochondrial membrane potential in winter wheat cells. Biochemistry (Mosc) 2014;79:1202–1210.
Gook DA, Edgar DH, Borg J, Archer J, McBain JC. Diagnostic assessment of the developmental potential of human cryopreserved ovarian tissue from multiple patients using xenografting. Hum Reprod 2005;20:72–78.
Gougeon A. Regulation of ovarian follicular development in primates: facts and hypotheses. Endocr Rev 1996;17:121–155.

Grynberg M, Poulain M, Sebag-Peyrelevade S, le Parco S, Fanchin R, Frydman N. Ovarian tissue and follicle transplantation as an option for fertility preservation. Fertil Steril 2012;97:1260–1268.
Huang L,MoY,WangW, LiY, Zhang Q,Yang D. Cryopreservation of human ovarian tissue by solid-surface vitrification. Eur J Obstet Gynecol Reprod Biol 2008;139:193–198.
Herraiz S, Novella-Maestre E, Rodrı´guez B, Dı´az C, Sa´nchez-Serrano M, Mirabet V, Pellicer A. Improving ovarian tissue cryopreservation for oncologic patients: slow freezing versus vitrification, effect of different procedures and devices. Fertil Steril 2014;101:775–784.
Isachenko V, Isachenko E,Weiss JM, Todorov P, Kreienberg R. Cryobanking of human ovarian tissue for anti-cancer treatment: comparison of vitrification and conventional freezing. Cryo Letters 2009;30:449–454.
Jeremias E, Bedaiwy MA, Nelson D, Biscotti CV, Falcone T. Assessment of tissue injury in cryopreserved ovarian tissue. Fertil Steril 2003;79:651–653.
Jeruss JS,Woodruff TK. Preservation of fertility in patients with cancer.NEng J Med 2009;360:902–911.
Kernohan KD, Be´rube´ NG. Three dimensional dual labelled DNA fluorescent in situ hybridization analysis in fixed tissue sections. MethodsX 2014;1:30–35.
Keros V, Xella S, Hultenby K, Pettersson K, Sheikhi M, Volpe A, Hreinsson J, Hovatta O. Vitrification versus controlled-rate freezing in cryopreservation of human ovarian tissue. Hum Reprod 2009;24:1670–1683.
Kim S, Agca C, Agca Y. Effects of various physical stress factors on mitochondrial function and reactive oxygen species in rat spermatozoa. Reprod Fertil Dev 2013;25:1051–1064.
Klocke S, Bu¨ndgen N, Ko¨ ster F, Eichenlaub-Ritter U, Griesinger G. Slow-freezing versus vitrification for human ovarian tissue cryopreservation. Arch Gynecol Obstet 2015;291:419–426.
Lepreux S, Guyot C, Billet F, Combe C, Balabaud C, Bioulac-Sage P, Desmoulie`re A. Smoothelin, a new marker to determine the origin of liver fibrogenic cells. World J Gastroenterol 2013;19:9343–9350.
Li YB, Zhou CQ, Yang GF,Wang Q, Dong Y. Modified vitrification method for cryopreservation of human ovarian tissues. Chin Med J (Engl) 2007; 120:110–114.
Martino NA, Dell’aquila ME, Cardone RA, Somoskoi B, Lacalandra GM, Cseh S. Vitrification preserves chromatin integrity, bioenergy potential and oxidative parameters in mouse embryos. Reprod Biol Endocrinol 2013;11:27.

Navarro-Costa P, Correia SC, Gouveia-Oliveira A, Negreiro F, Jorge S, Cidada˜o AJ, Carvalho MJ, Plancha CE. Effects of mouse ovarian tissue cryopreservation on granulosa cell-oocyte interaction. Hum Reprod 2005;20:1607–1614.
Oktem O, Alper E, Balaban B, Palaoglu E, Peker K, Karakaya C, Urman B. Vitrified human ovaries have fewer primordial follicles and produce less antimullerian hormone than slow-frozen ovaries. Fertil Steril 2011; 95:2661–4.e1.
Pan J, Thoeni C, Muise A, Yeger H, Cutz E. Multilabel immunofluorescence and antigen reprobing on formalin-fixed paraffin-embedded sections: novel applications for precision pathology diagnosis. Mod Pathol 2016; 1–13. [Epub ahead of print].
Rahimi G, Isachenko E, Sauer H, Isachenko V,Wartenberg M, Hescheler J, Mallmann P, Nawroth F. Effect of different vitrification protocols for human ovarian tissue on reactive oxygen species and apoptosis. Reprod Fertil Dev 2003;15:343–349.
Rahimi G, Isachenko V, Todorov P, Tawadros S, Mallmann P, Nawaroth F, Isachenko E. Apoptosis in human ovarian tissue after conventional freezing or vitrification and xenotransplantation. Cryo Letters 2009;30:300–309.
Rahimi G, Isachenko V, Kreienberg R, Sauer H, Todorov P, Tawadros S, Mallmann P, Nawroth F, Isachenko E. Re-vascularisation in human ovarian tissue after conventional freezing or vitrification and xenotransplantation. Eur J Obstet Gynecol Reprod Biol 2010;149:63–67.
Rai V, Dey N. The Basics ofConfocal Microscopy, Laser Scanning, Theory and Applications, Prof. Chau-Chang Wang (Ed.), ISBN:978-953-307-205-0 2011 InTech, Available from: http://www.intechopen.com/books/laserscanning- theory-and-application/the-basics-of-confocal-microscopy. Ch. 5: pp 75–96.
Robertson D, Isacke CM. Multiple immunofluorescence labeling of formalin-fixed paraffin-embedded tissue. Methods Mol Biol 2011; 724:69–77.
Sanfilippo S, Canis M, Smitz J, Sion B, Darcha C, Janny L, Brugnon F. Vitrification of human ovarian tissue: a practical and relevant alternative to slow freezing. Reprod Biol Endocrinol 2015;13:67.
Santana LN, Van den Hurk R, Oskam IC, Brito AB, Brito DC, Domingues SF, Santos RR. Vitrification of ovarian tissue from primates and domestic ruminants: an overview. Biopreserv Biobank 2012;10:288–294.
Schover LR. Patient attitudes toward fertility preservation. Pediatr Blood Cancer 2009;53:281–284.
Stempel AJ, MorgansCW, Stout JT, Appukuttan B. Simultaneous visualization and cell-specific confirmation ofRNAand protein in the mouse retina. Mol Vis 2014;20:1366–1373.

Suzuki N, Yoshioka N, Takae S, Sugishita Y, Tamura M, Hashimoto S, Morimoto Y, Kawamura K. Successful fertility preservation following ovarian tissue vitrification in patients with primary ovarian insufficiency.Hum Reprod 2015;30:608–615.
Talevi R, Barbato V, Fiorentino I, Braun S, De Stefano C, Ferraro R, Sudhakaran S, Gualtieri R. Successful slush nitrogen vitrification of human ovarian tissue. Fertil Steril 2016;S0015-0282(16)00084-4.
Wang Q, Tian S,Wang Q, Huang Q, Yang J. Melting characteristics during the vitrification of MSWI fly ash with a pilot-scale diesel oil furnace. J Hazard Mater 2008a;160:376–381.
Wang Y, Xiao Z, Li L, FanW, Li SW. Novel needle immersed vitrification: a practical and convenient method with potential advantages in mouse and human ovarian tissue cryopreservation. Hum Reprod 2008b; 23:2256–2265.
Wang TR, Yan J, Lu CL, Xia X, Yin TL, Zhi X, Zhu XH, Ding T, Hu WH, Guo HY et al. Human single follicle growth in vitro from cryopreserved ovarian tissue after slow freezing or vitrification. Hum Reprod 2016; 31:763–773.
Xiao Z,Wang Y, Li L, Luo S, Li SW. Needle immersed vitrification can lower the concentration of cryoprotectant in human ovarian tissue cryopreservation. Fertil Steril 2010;94:2323–2328.
Zhou XH, Wu YJ, Shi J, Xia YX, Zheng SS. Cryopreservation of human ovarian tissue: comparison of novel direct cover vitrification and conventional vitrification. Cryobiology 2010;60:101–105.
Zucker RM, Jeffay SC. Confocal laser scanning microscopy of whole mouse ovaries: excellent morphology, apoptosis detection, and spectroscopy. Cytometry A 2006;69:930–939.